Journal of Microencapsulation
Micro and Nano Carriers

ISSN: 0265-2048 (Print) 1464-5246 (Online) Journal homepage: https://www.tandfonline.com/loi/imnc20

Impact of storage on the physico-chemical properties of microparticles comprising a hydrogenated vegetable oil matrix and different essential oil concentrations

Pia Gottschalk, Benjamin Brodesser, Denis Poncelet, Henry Jaeger, Harald Rennhofer & Stephen Cole

To cite this article: Pia Gottschalk, Benjamin Brodesser, Denis Poncelet, Henry Jaeger, Harald Rennhofer & Stephen Cole (2019) Impact of storage on the physico-chemical properties of microparticles comprising a hydrogenated vegetable oil matrix and different essential oil concentrations, Journal of Microencapsulation, 36:1, 72-82, DOI: 10.1080/02652048.2019.1599456

To link to this article: https://doi.org/10.1080/02652048.2019.1599456

JOURNAL OF MICROENCAPSULATION
2019, VOL. 36, NO. 1, 72–82
https://doi.org/10.1080/02652048.2019.1599456

Taylor & Francis
Taylor & Francis Group

REVIEW

Impact of storage on the physico-chemical properties of microparticles comprising a hydrogenated vegetable oil matrix and different essential oil concentrations

Pia Gottschalk[a,b,c], Benjamin Brodesser[c], Denis Poncelet[a], Henry Jaeger[b], Harald Rennhofer[d] and Stephen Cole[c]

[a]Oniris, UMR CNRS 6144 GEPEA, Nantes, France; [b]University of Natural Resources and Life Sciences, Vienna, Austria; [c]Biomin Research Centre, Tulln, Austria; [d]University of Natural Resources and Life Sciences, Vienna, Austria

ABSTRACT

Microparticles made from hydrogenated sunflower oil without essential oil and with different essential oil concentrations (75–300 g/kg; g of essential oil per kg of microparticles) were stored for 1 or 2 months at 25 or 37 °C. Before and after storage the essential oil concentration, flowability, optical appearance, melting behaviour and crystalline structure of the microparticles were investigated. Essential oil recovery, melting behaviour and crystalline structure were identical for the essential oil containing microparticles and were not affected during storage. The surface structure of the microparticles varied with their essential oil concentration. While the particles containing 75 g/kg essential oil were covered by erect fat crystals, those with 225 g/kg and higher were mostly smooth with some round shaped dumps. However, the surface of all essential oil containing microparticle batches had reached their final stage after production already and did not change during storage. Microparticles without essential oil presented two melting peaks; all microparticle batches with essential oil had one peak. Peaks in the X-ray scattering powder diffraction signal of the essential oil-free microparticles after production can be associated with the α-form of the hydrogenated vegetable oil. During storage, a conversion of the α-form to the stable β-form was observed. Microscopy showed that these microparticles also developed strong fat crystals throughout storage. The triglycerides in microparticles with essential oil seem to directly take on the stable β-form. The formation of robust microparticle agglomerates during storage was prevalently observed for the fat crystal forming product batches, meaning the products without or with low essential oil concentration.

ARTICLE HISTORY
Received 12 October 2018
Accepted 21 March 2019

KEYWORDS
Essential oil; matrix encapsulation; hydrogenated vegetable fat; storage stability; surface structure; polymorphic transition

1. Introduction

Essential oils have become widely used as additives or supplements in animal feed due to their antimicrobial, antifungal, and antiviral effects (Bento *et al*. 2013, El Asbahani *et al*. 2015). This development was further promoted by the need to eliminate antibiotics in animal nutrition and the positive effect of essential oils on the animals' growth performance, gut microbiota, and welfare (Murugesan *et al*. 2015, Zeng *et al*. 2015, Suresh *et al*. 2018).

Their volatile character and their tendency to oxidation make the protection of essential oils from environmental influences inevitable. Furthermore, the intensive odour and taste of essential oils in many cases require masking to optimally increase their acceptance by humans and animals (Blake and Attwool 1998, Arun *et al*. 2011, Dolçà *et al*. 2015, Turasan *et al*. 2015)

Microencapsulation is a technology widely used in diverse industries, such as the pharmaceutical, food, and feed industry to mask inacceptable flavours, protect the encapsulated ingredients from environmental influences, control their release, or convert liquid ingredients into solids (Nedovic *et al*. 2011, Jyothi *et al*. 2012). It covers all processes from which particles in the micrometre scale up to 1 mm entrapping at least one active ingredient are formed (Jyothi *et al*. 2010). Depending on the applied technique, the active ingredient is either finely dispersed within the inert matrix material (matrix encapsulation) or surrounded by a solid material layer (core–shell encapsulation). The decision on whether the active compound is

CONTACT Pia Gottschalk pia.gottschalk@biomin.net Biomin Research Centre, Technopark 1, 3430 Tulln, Austria

matrix encapsulated or surrounded by a solid layer depends largely on the aspired product properties (Gibbs *et al*. 1999). Core–shell encapsulation is applied when the active ingredients need full protection from environmental influences and when instantaneous release is required. Sustained release of the active ingredient can be performed by matrix encapsulation. Typical methods for matrix encapsulation are spray drying and spray-chilling. Typical methods for core–shell encapsulation are fluidised-bed coating and pan coating.

The most common methods for encapsulation of essential oils are spray drying, (co-) extrusion, and coacervation (Martins *et al*. 2009, Dolçà *et al*. 2015, Kausadikar *et al*. 2015). In spray drying, the aqueous mixture of active ingredient and matrix material is atomised and water evaporates at temperatures around 200 °C. Characteristics for the produced powders are reduced flowability and satisfying water solubility. In co- (extrusion), microparticles are formed by cutting a laminar fluid flow under the impact of an overlap vibration. Coacervation is characterised by entrapment of an active ingredient as the result of network formation of either one (simple coacervation) or two charged (complex coacervation) water soluble polymers.

Two exemplary encapsulation methods in which waxes or hydrogenated vegetable oils are used as encapsulating agent are hot melt coating and spray-chilling/prilling. In hot melt coating, the solid carrier particles are covered with a coating while being fluidised in the process chamber of a fluidised bed plant (Jozwiakowski *et al*. 1990, Dewettinck and Huyghebaert 1999). Spray-chilling is a gentle matrix encapsulation process, in which the active ingredients are dispersed within the hydrophobic matrix material. When atomised into a cooled process room the material droplets harden to microparticles (Nedovic *et al*. 2011, Okuro *et al*. 2013, Vervaeck *et al*. 2013).

Using hydrogenated vegetable oils for product formulation purposes, changes in their physical properties during processing and storage must be taken into account. The reason for this is that triglycerides can take on diverse polymorphic forms with the α-form being the least stable and the β-form being the most stable one (Mayama 2009). Additionally, intermediate β′-forms can occur (Sato 2001, Himawan *et al*. 2006). These polymorphic forms can transform into each other from the α- over the β′ to the β-form. The velocity of polymorphic transformation can actively be influenced by the presence of additives such as surfactants and essential oils but also by exposure to elevated temperatures. This in turn, can lead to the formation of fine fat flakes on the surface of fat-based formulations. Due to their similarity to petals of flowers, these fat flakes are also known as fat blooming (Lopes *et al*. 2015, Miyasaki *et al*. 2016).

Since the exposure of feed additives to elevated temperatures above room temperature during transport and storage cannot be excluded, the application of newly developed fat-based feed additives needs to be investigated due to polymorphic transformation and fat blooming and their impact on the storage stability of the formulations. In a previous study, it was already demonstrated by Gottschalk *et al*. (2018) that the essential oil concentration in fat-based microparticles has an impact on the physico-chemical properties of the same and the occurrence of fat blooming.

The aims of the present study were to investigate the impact of the initial essential oil concentration and the storage conditions on the physico-chemical properties, such as surface structure, flowability, and crystallinity, of fat-based, essential oil containing microparticles. Additionally, it was of interest whether differences in the surface structure, detected directly after production, have an impact on the mid-term storability of the different microparticles.

2. Materials and methods

2.1. Chemicals and consumables

Hydrogenated vegetable oil (VGB 5 ST; melting point 69–73 °C; stearic acid (18:0) ≥90%, palmitic acid (16:0) ≥7%, together with oleic acid (18:1), arachidic acid (20:0), behenic acid (22:0); CAS: 91082–37-0) was purchased from ADM Sio (Fourqueux, France). The essential oil mixture used as the active ingredient was a proprietary blend (major component (70% v/v) carvacrol together with thymol, carvone, and linalool) from Biomin® Phytogenics GmbH (Stadtoldendorf, Germany). The sachets (Art. Nr. 2020–0226; 160 mm × 230 mm) made from glue-laminated aluminium compound foil (Polyethylene terephthalate 12 μm/aluminium 9 μm/polyethylene 90 μm) used for the storage trial were purchased from Sokufol Folien GmbH (Limburg an der Lahn, Germany).

2.2. Preparation of microparticles

Hydrogenated vegetable oil was heated on a digital magnetic stirrer (IKA Model RCTB, IKA-Werke GmbH & Co, Staufen, Germany) to 85 °C until molten and different amounts of the essential oil mixture were added with continuous mixing (300 rpm). The molten material mixtures were atomised by spinning disc (6 cm

diameter, 2000–3000 rpm, Sprai SAS, Orsay, France) and solidified by cooling at room temperature in a self-constructed process chamber (approx. $2 \times 2 \times 2$ m). Microparticles were collected at a controlled distance, indicated by the spinning disc controlling software, from the centre of the atomiser.

2.3. Storage of microparticles

200 g of the microparticles were filled into heat-sealed sachets. The sachets were stored at either 25 °C or 37 °C for 1 or 2 months in an incubator (BF 240, Binder, Tuttlingen, Germany). For each sampling point, 200 g of the material were filled into an individual sachet so that storage of the 2 month batches did not have to be interrupted when the 1 month batches were taken. Analysis was performed subsequent to sampling.

2.4. Microparticle characterisation

2.4.1. Powder flowability

Powder flowability was determined by angle of repose measurement. Microparticles were poured through a glass funnel onto a disc ($r = 3$ cm) positioned 15 cm below. The height of the emerging cone (h in cm) was determined and the angle of repose (α) was obtained using the equation:

$$\tan \alpha = \frac{h}{r} \tag{1}$$

Empirical powder flowability was determined from the angle of repose (Lumay *et al*. 2012). Every determination was performed in triplicate.

2.4.2. Total retention efficiency

The concentration of the main essential oil compounds, linalool, carvone, thymol, and carvacrol, making up ≥90% of the essential oil mixture imbedded in the microparticles was determined with a Shimadzu GC 2010 (Shimadzu, Austria) gas chromatograph with a FID detector and an Optima WAX plus (Machery-Nagel, Germany) column, 30 m length, 0.25 mm id. From these concentrations, the total retention efficiency, defined as the sum of essential oil recovered in the microparticle matrix and on the surface of the same, was calculated. For extraction of the essential oil, 0.1–0.11 g of microparticles were intensively mixed with 1.5 mL ethyl acetate (Chem Labs, Bartelt, Graz, Austria), centrifuged (4000 rpm), and the supernatant was collected for analysis. The extraction was repeated three times. The instrument was operated with helium as carrier gas (1.2 mL/min). The oven programme started at 60 °C for 1 min, 5 °C/min–85 °C, 25 °C/min–150 °C, 6 °C/min–200 °C, 30 °C/min–270 °C hold 7 min. The FID detector was operated at 280 °C with a flow of hydrogen of 40 mL/min, air 400 mL/min, and He as makeup gas 30 mL/min. The data rate was 25 Hz. The concentration of the single essential oil compounds in a product batch was determined by integration and comparison of the real and the theoretical peak area.

Knowing the essential oil concentration in the microparticles and the theoretically expected essential oil concentration, the total retention efficiency could be calculated using the following formula.

$$\text{Total retention efficiency } [\%] = \frac{\text{Essential oil concentration in the particles } \left[\frac{\text{mg}}{\text{g}}\right]}{\text{Theoretical essential oil concentration } \left[\frac{\text{mg}}{\text{g}}\right]} * 100 \tag{2}$$

2.4.3. Structural and morphological analysis

The surface of the microparticles was investigated by light microscopy and scanning electron microscopy. Light microscopy was performed with a Leica M80 (Leica, Vienna, Austria) stereomicroscope. Scanning electron microscopy analysis was either done with a Zeiss Supra 35 (Carl Zeiss Microscopy GmbH, Jena, Germany) or with a Quanta FEG 250 (FEI, Oregon, U.S.A). The images were recorded with the SE detector with a beam voltage of 3 or 5 kV, a beam current of 80 μA, and a spot size of 1–2 nm. The working distance was 5 mm. Samples investigated by scanning electron microscopy were either sputtered with carbon in a rotor Emitech K950x (Emitech, Maine, USA) vacuum coater or with gold in a HHV Scancoat Six (HHV, Bangalore, India) compact sputter coater.

2.4.4. Investigation of the melting behaviour

The melting behaviour was investigated by differential scanning calorimetry. Analysis was performed with a STA 449 F1 calorimeter (Netzsch, Selb, Germany) and the data evaluation with the Netzsch Proteus Thermal Analysis software Version 5.2.1. All measurements were done in closed aluminium crucibles. Melting curves were determined at a standard heating rate of 10 K/min, which allows the clear expression of the melting peaks, between −50 and 90 °C. Each measurement consisted of two melting cycles. Helium with a flow rate of 40 mL/min was used as purging gas. Calibration of the equipment was performed with

adamantane, zinc, tin bismuth, and indium. The sample weight for all measurements was 10 ± 0.6 mg.

2.4.5. Investigation of the crystalline structure

X-ray powder diffraction scattering was performed with a Rigaku SMax3000 (Rigaku, Tokyo, Japan) with a Triton200 (Rigaku, Tokyo, Japan) multiple wire detector for the small angle X-ray scattering and a Fuji Image Plate (Fuji, Tokyo, Japan) for wide angle X-ray diffraction. The wide angle X-ray scattering images were recorded in one single shot of 1800 s exposure time in the range of 1–4.5 $Å^{-1}$ (corresponding to 14–67 degree scattering angle) and the Fuji Image Plate was read out with a resolution of 0.0453 degrees scattering angle. The small angle X-ray scattering images were also recorded in one single shot but for 3600 s each in the range of 0.01–1 $Å^{-1}$. A MM002+ micro focus X-ray tube with copper target (Cu-K_α, wavelength 0.154 nm) and integrated confocal max-flux small angle X-ray scattering optics (Rigaku) was operated with 45 kV and 0.88 mA. The system uses a 3-pinhole collimation to obtain a circular beam of about 210 μm diameter on the sample. For the sample preparation, a small amount of the microparticles was fixed between two plastic stripes. The signal from the plastic stripes alone was subtracted from the signals coming from the samples to eliminate the background signal.

3. Results and discussion

3.1. Storage of microparticles

Five microparticle batches with essential oil concentrations ranging from 0 to 300 g/kg were stored for 1 or 2 months at 25 or 37 °C in heat-sealed sachets made from glue-laminated aluminium compound foil, each of which contained 200 g of microparticles. After storage the flow properties, surface structure, total retention efficiency, melting behaviour, and crystallinity were determined.

3.2. Powder flowability

After production, all microparticle batches were available as free-flowing powders with the flowability getting worse as function of the essential oil concentration. This observation was in good correlation with the data presented by Yang and Ciftci (2016) who observed the formation of particle agglomerates with increasing peppermint oil concentration in their liquid filled nanoparticles. The flowability of microparticles without essential oil was excellent throughout storage at 25 °C but formed robust aggregates when stored at 37 °C. The microparticles with 75 g/kg essential oil agglomerated under all tested storage conditions. With essential oil concentrations of 150 g/kg and higher the microparticles remained free-flowing. The flowability of microparticles with 225 g/kg and 300 g/kg essential oil was stable during storage. After storage at 37 °C, the flowability of these microparticles was fair or even excellent (angle of repose values between 27.5° and 36°).

Additional analysis was performed to identify the reason for changes in flowability and the variations between the different batches.

3.3. Appearance and surface structure

Light microscopy revealed that changes in the surface structure of fat-based microparticles during storage depended on their essential oil concentration (Figure 1). While microparticles without essential oil turned opaque during storage, especially at 37 °C, microparticles with 75 g/kg essential oil were opaque after production already and did not change their appearance. Microparticles with 150–300 g/kg essential oil kept their transparency from production and throughout storage.

Scanning electron microscopy showed that the opaque appearance of the microparticles was the result of erect fat flakes on the surface of the microparticles, known as fat blooming (Bricknell and Hartel 1998, De Graef *et al*. 2005, Mayama 2009). Their occurrence was strongly dependent on the initial essential oil concentration of the microparticles and the storage conditions.

Microparticles without essential oil tended to develop fat blooming when stored at 37 °C and were covered by erect fat flakes after 2 months. When stored at 25 °C, fat flake formation was slower. The observation that the formation of fat blooming is a function of temperature and time is supported by a study from Lopes *et al*. (2015) in which anhydrous citric acid was coated with tristearin. Fat blooming was enhanced when the particles were stored at 50 °C and X-ray scattering powder diffraction confirmed that the development of fat blooming was a result of polymorphic transformation of tristearin from its less stable α-form to the stable β-form.

In the presence of essential oil, the formation of stable surface structures was accelerated and changes during storage were negligible, independent of the initial essential oil concentration, storage temperature, and time. While the surface of microparticles with 75 g/kg essential oil remained flaky, the surface of microparticles with 150 g/kg essential oil and higher

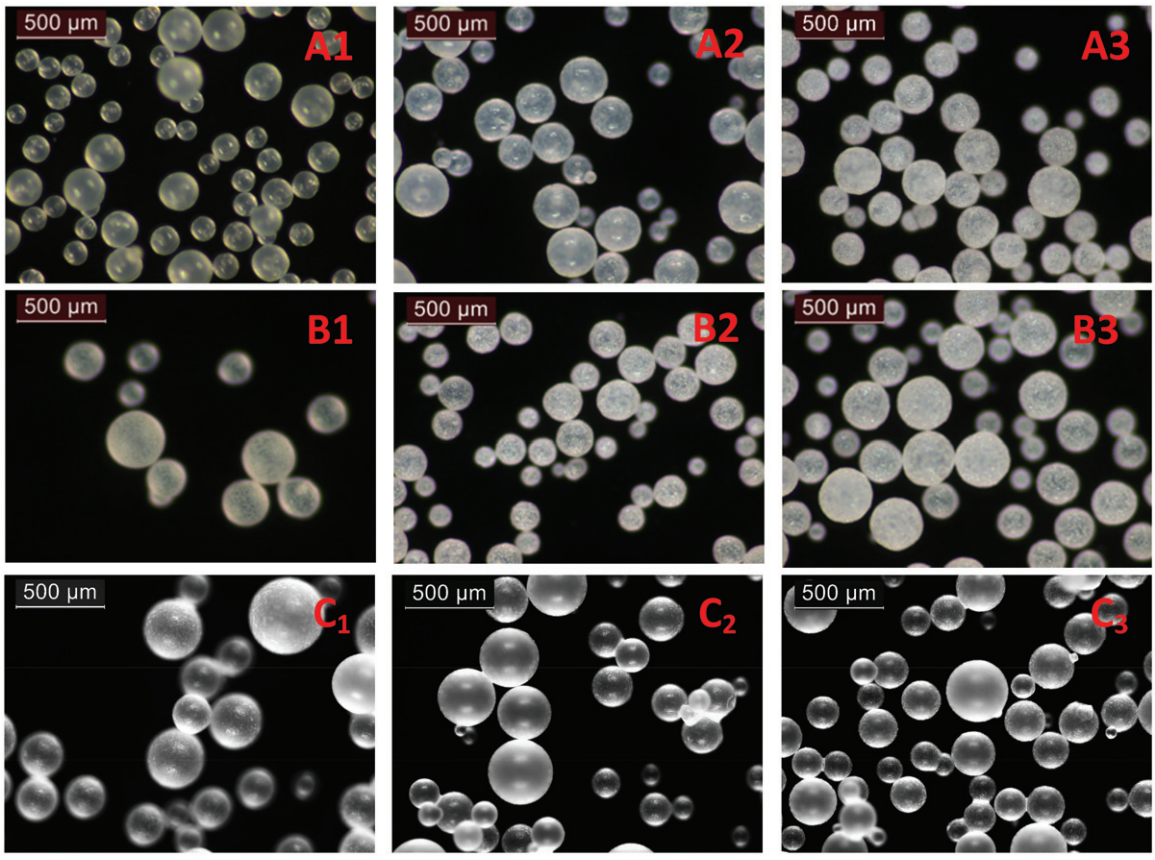

Figure 1. Light microscopy of microparticles without essential oil (A), with 75 g/kg (B) and 300 g/kg (C) essential oil directly after production (1), after 2 months storage at 25 °C (2), and after 2 months storage at 37 °C (3).

was still smooth with isolated flakes or protrusions (Figure 2). In the chocolate industry, this effect is associated with the polymorphic transformation of tristearin to its β-form being supported in the presence of essential oils (e.g. limonene) (Miyasaki *et al*. 2016, Rigolle *et al*. 2016) and other liquid compounds.

Blooming observed on the surface of microparticles with 75 g/kg essential oil may be a result of fat migration and its recrystallization. This type of fat blooming is often observed in filled chocolate, in which the liquid lipid fraction and the solid crystals of the filling migrate through the surrounding chocolate to its surface, where they recrystallizes (Ziegleder and Schwingshandl 1998, De Graef *et al*. 2005).

Yang and Ciftci (2016) associated changes in the surface structure of peppermint-oil loaded nano- and microparticles with an increased release of the encapsulated essential oils from core–shell capsules during storage. Fat blooming was mostly pronounced for microparticles with 50 and 100 g/kg essential oil in scanning electron microscopic pictures. These microparticle batches furthermore showed the highest essential oil release. Also by scanning electron microscopy we showed that storage at 37 °C but also 25 °C for 2 months had the strongest impact on the surface of microparticles without essential oil. In consideration of this result fat blooming cannot exclusively be traced to essential oil evaporation and the observations made by Yang and Ciftci could not be confirmed.

Aggregation is reversible by the application of mechanical force. Since aggregation caused by melting of microparticles would be irreversible, this observation supports the theory of fat flake entanglement on the surface of microparticles without and with 75 g/kg essential oil being the reason for agglomeration. This assumption is furthermore supported by the observation that microparticles with essential oil concentrations above 150 g/kg and without fat flakes on their surface remain free-flowing throughout the whole storage trial. Slightly pronounced irregularities on the surface of these microparticles further stabilise their flow behaviour by reduction of the direct contact area between the single particles.

3.4. Essential oil recovery

The concentrations of the four main essential oil compounds, linalool, carvone, thymol, and carvacrol, were hardly affected during storage (Figure 3). The only compound whose concentration decreased slightly in

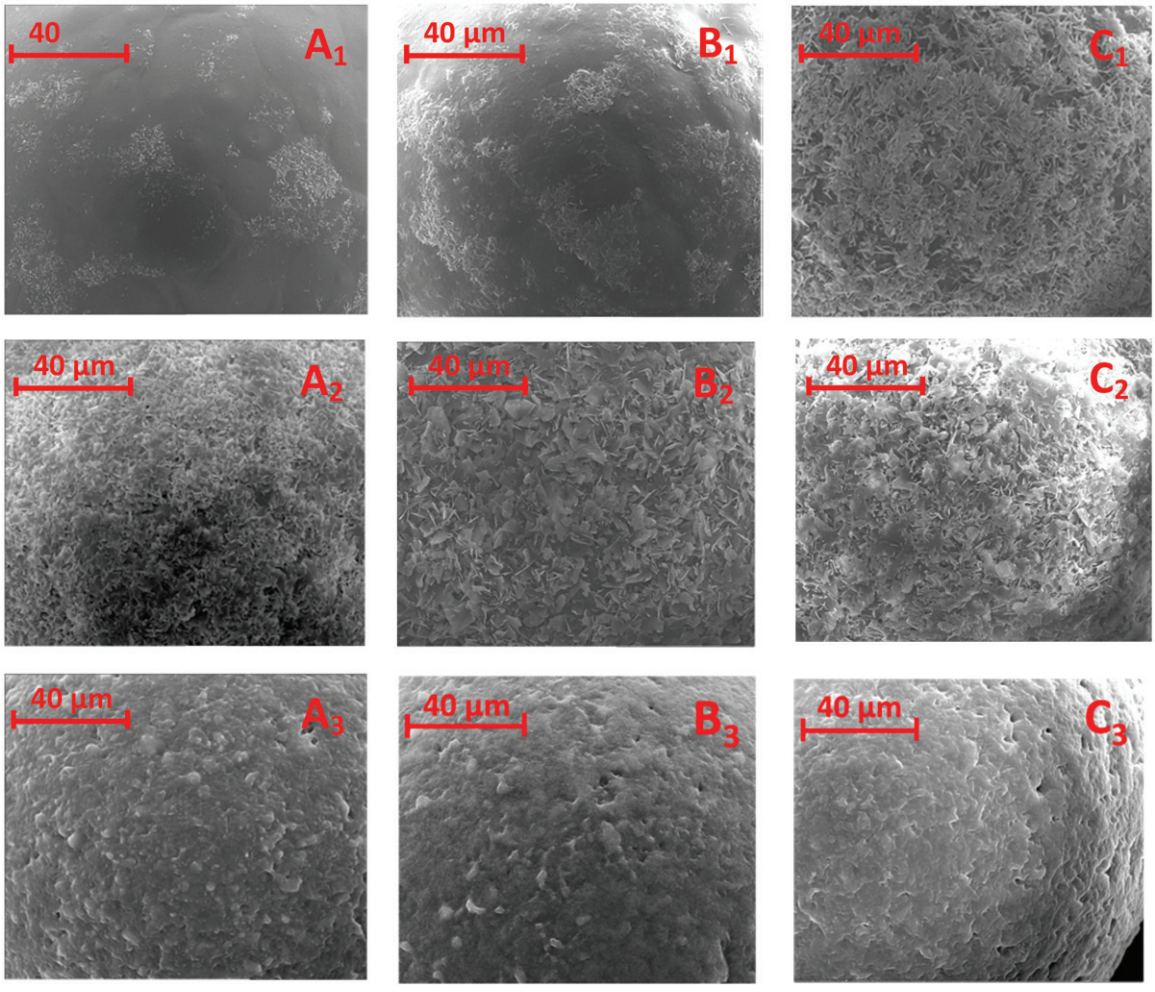

Figure 2. Scanning electron microscopy picture of the microparticles without (A_1–C_1), with 75 g/kg (A_2–C_2) and with 300 g/kg (A_3–C_3) essential oil after production (A), and after 2 months storage at 25 °C (B) and 37 °C (C).

all microparticle batches was linalool. With down to 86% recovery it was already the least stable compound after the encapsulation process. Carvone and thymol had similar stabilities with maximum losses of 8 or 6%. Carvacrol was not affected at all during storage. With linalool having the highest vapour pressure (0.17 mmHg @ 25 °C) it has the strongest tendency to evaporate. Carvacrol, conversely, has the lowest vapour pressure (0.0177 mmHg @ 25 °C) and is expected to be more stable than the other compounds. This tendency was already observed after production.

In contrast to the theory established by Yang and Ciftci (2016) that fat blooming is a result of increased essential oil evaporation all microparticle batches investigated in the present study showed constant essential oil recoveries throughout storage. Consequently, fat blooming on the surface of hydrogenated vegetable oil-based microparticles with 75 g/kg essential oil cannot be attributed to excessive essential oil reduction. Another possible reason for the occurrence of fat blooming on the surface of these microparticles could be the polymorphic transformation of triglycerides from the least stable α-form to the stable β-form (Miyasaki *et al*. 2016), which can be investigated by melting profile and crystallinity investigations.

3.5. Melting behaviour

For microparticles without essential oil differential scanning calorimetric measurements resulted in melting curves with transitions at 57 °C (Tm_{max1}) and 69 °C (Tm_{max2}) and a 5.5 times higher melting enthalpy at lower temperature (ΔHm_1) than at higher temperature (ΔHm_2) after production. This profile changed slightly during storage at 25 °C. When stored at 37 °C, the transitions remained in the same temperature ranges with $Tm_{max1} = 57\,°C \pm 1\,°C$ and $Tm_{max2} = 69\,°C \pm 4\,°C$, however, the enthalpy ratio was reversed with ΔHm_2

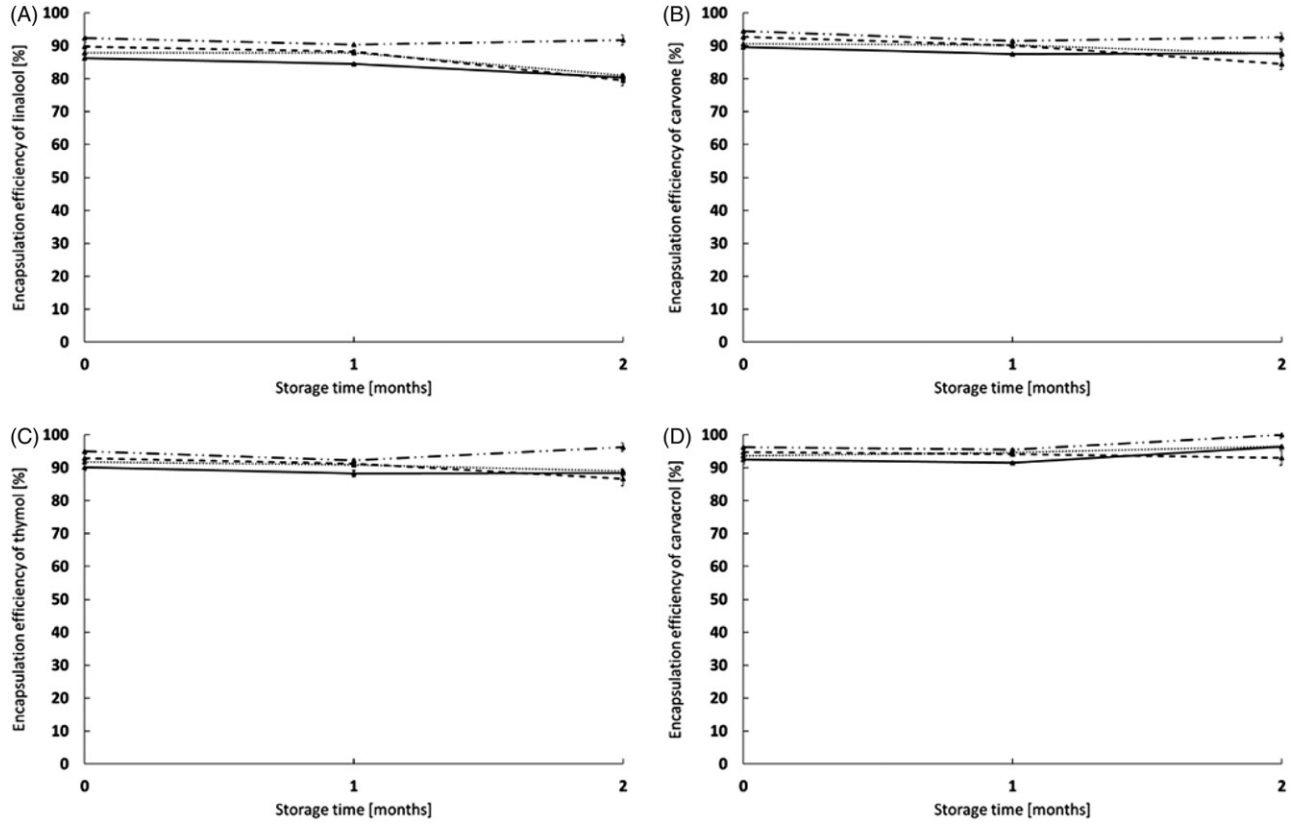

Figure 3. Encapsulation efficiency of the essential oil compounds linalool (A), carvone (B), thymol (C), and carvacrol (D) in the various microparticle batches after production and after 1 or 2 months storage at 37 °C. With (—·) representing the microparticles with 300 g/kg, (— —) with 225 g/kg, (·····) with 150 g/kg and (—) with 75 g/kg essential oil ($n = 2$).

increasing from 15% to more than 80% of total enthalpy (Figure 4).

The two transition peaks are an indication for the presence of different polymorphic forms of tristearin. This was already discussed by Schoenitz *et al.* (2014) who tried to control the polymorphic transformation of continuously crystallized solid lipid nanoparticles. The transition shift throughout storage in favour of the peak at higher temperature, furthermore indicates that the first peak represents the least stable α-polymorphic form and the second peak one of the more stable β′- or β-forms (Nassu and Gonçalves 1999).

The melting curves of the essential oil containing microparticles exhibited one transition only (data were shown in Gottschalk *et al.* 2018), characterised by its melting peak maximum (Tm_{max}) and the melting enthalpy (ΔHm). The essential oil concentration had an impact on the melting behaviour of the microparticles with Tm_{max} values decreasing with increasing essential oil concentration. Storage for a maximum of 2 months had no effect on the melting behaviour of microparticles containing essential oil (Table 1).

The presence of essential oil had a stabilising effect on the melting behaviour of spray-chilled microparticles.

3.6. Crystallinity

X-ray scattering powder diffraction was performed to investigate the crystalline structure of microparticles and the impact of essential oil, storage time, and temperature.

When stored at 25 °C, the SAXS and the WAXS signals of microparticles without essential oil changed slightly. The area of the main peaks in the SAXS signal at 0.124 $Å^{-1}$ (q_{01}), 0.28 $Å^{-1}$ (q_{02}), and 0.36 $Å^{-1}$ (q_{02}), corresponding to the (001), (002), and (003) spectrum of a double chain-length structure (Takeuchi *et al.* 2002), decreased. The main peak in the WAXS signal at 1.58 $Å^{-1}$, corresponding to a hexagonal arrangement of the short-range order of the α-polymorphic form of tristearin, shifted to the left. Storage of the same product at 37 °C resulted in obvious changes with the main peaks of the SAXS signal and the peak in the WAXS signal, dividing into several peaks (Figure 5 A_1 and B_1). Furthermore, the sustained, convex WAXS signal began to exhibit small peaks (Figure 5 B_1 (black circle)).

The crystalline structure of the essential oil containing microparticles did not change during storage. Both the SAXS and the WAXS had peaks identical to

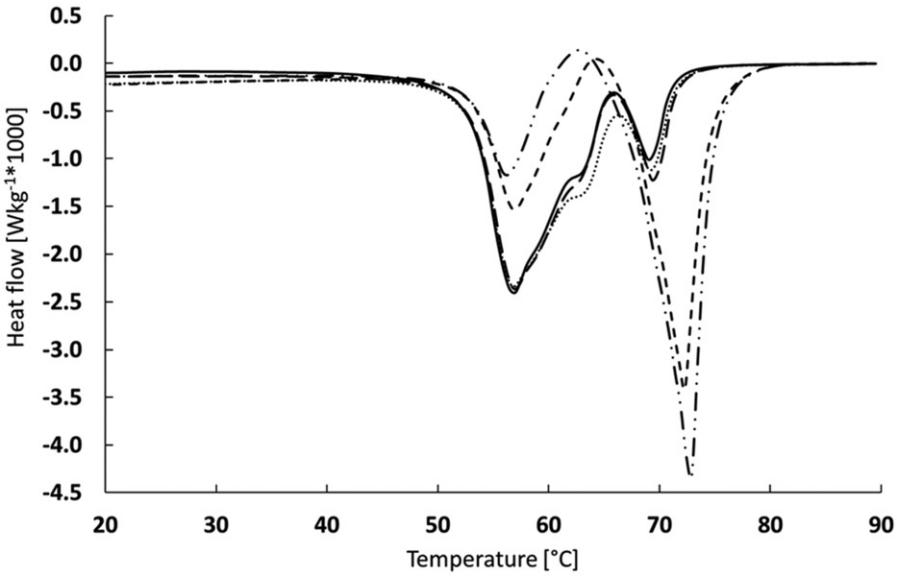

Figure 4. Melting behaviour of microparticles without essential oil after production (—) and after one month storage at 25 °C (·····) or 37 °C (− −) and after two months storage at 25 °C (— −) or 37 °C (−·). For the number of repetitions see Table 1.

Table 1. Melting maxima and transition enthalpies of the essential oil containing microparticles at day zero and after storage for 1 or 2 months. **(With *: $n = 1$ and **: $n = 2$).**

	Day 0		1 month		2 months	
Essential oil [g kg^{-1}]	Tm_{max} [°C]*	ΔHm [J/g]*	Tm_{max} [°C]**	ΔHm [J/g]**	Tm_{max} [°C]**	ΔHm [J/g]**
75	71.0	176	70.5 ± 0.1	175.5 ± 2.5	70.9 ± **0.0**	181 ± **0.0**
150	68.1	176	67.9 ± 0.1	150 ± **0.0**	68.2 ± **0.0**	172 ± **0.0**
225	65.8	154	65.4 ± 0.3	146 ± 2.0	65.2 ± 0.1	149.5 ± 1.5
300	62.9	143	62.7 ± 0.2	134 ± 1.0	62.7 ± 0.4	140 ± 2.0

the signal that had been gained after production. In Figure 5 A_2 and B_2, the respective signals gained for microparticles with 75 g/kg essential oil are shown. Also in the SAXS and WAXS signals of stored microparticles with higher essential oil content, no changes were observed.

Comparison of the SAXS and the WAXS signals makes evident that shifted and newly developed peaks of microparticles without essential oil after storage at 37 °C had equal positions to the main peaks of the microparticles with essential oil (Figure 5). The main SAXS signal (0.13 Å^{-1}) after 1 month storage at 37 °C of microparticles without essential oil exhibited a second maximum. This second maximum was at the same position (0.14 Å^{-1}) as the first scattering vector (q_{01}) of the microparticles with essential oil. Knowing q_{01} the thickness (d) of the lamellar structure could be calculated with $d = 2*\pi/q_{01}$ (Lopes *et al.* 2015). For the products with essential oil and the microparticles without essential oil after storage at 37 °C this yielded in a lamellar thickness of 44.86 Å^{-1}, representing the β-polymorphic form of tristearin. Before storage, the first scattering vector of microparticles without essential oil was at 0.124 Å^{-1} representing a lamellar thickness of 50.65 Å^{-1}, which corresponds to the α-polymorphic form of tristearin. In the WAXS signal of microparticles without essential oil the initial peak at 1.58 Å^{-1} decreased and new peaks at 1.21, 1.39, and 1.7 Å^{-1} formed. These new peaks were also identical to the peaks in the WAXS signal of the microparticles with essential oil.

The constant X-ray scattering powder diffraction signal of microparticles with essential oil and the assimilating signal of microparticles without essential oil fit well with the differential scanning calorimetric results. Quick solidification of pure hydrogenated vegetable oil results in the triglycerides adopting the less stable polymorphic α-form. The velocity of the transformation to the stable β-form is temperature dependent. In the presence of essential oil, the triglycerides take on the β-form directly after solidification. This result is in accordance with a study performed by Miyasaki *et al.* (2016) who found out that the polymorphic transformation in cacao butter and cacao butter equivalent was accelerated when stored at 25 °C in the presence of D-limonene in concentrations of 15–50 g/kg. Rigolle *et al.* (2016) came to the same conclusion when cacao butter with and without limonene was stored at 17 °C and 20 °C.

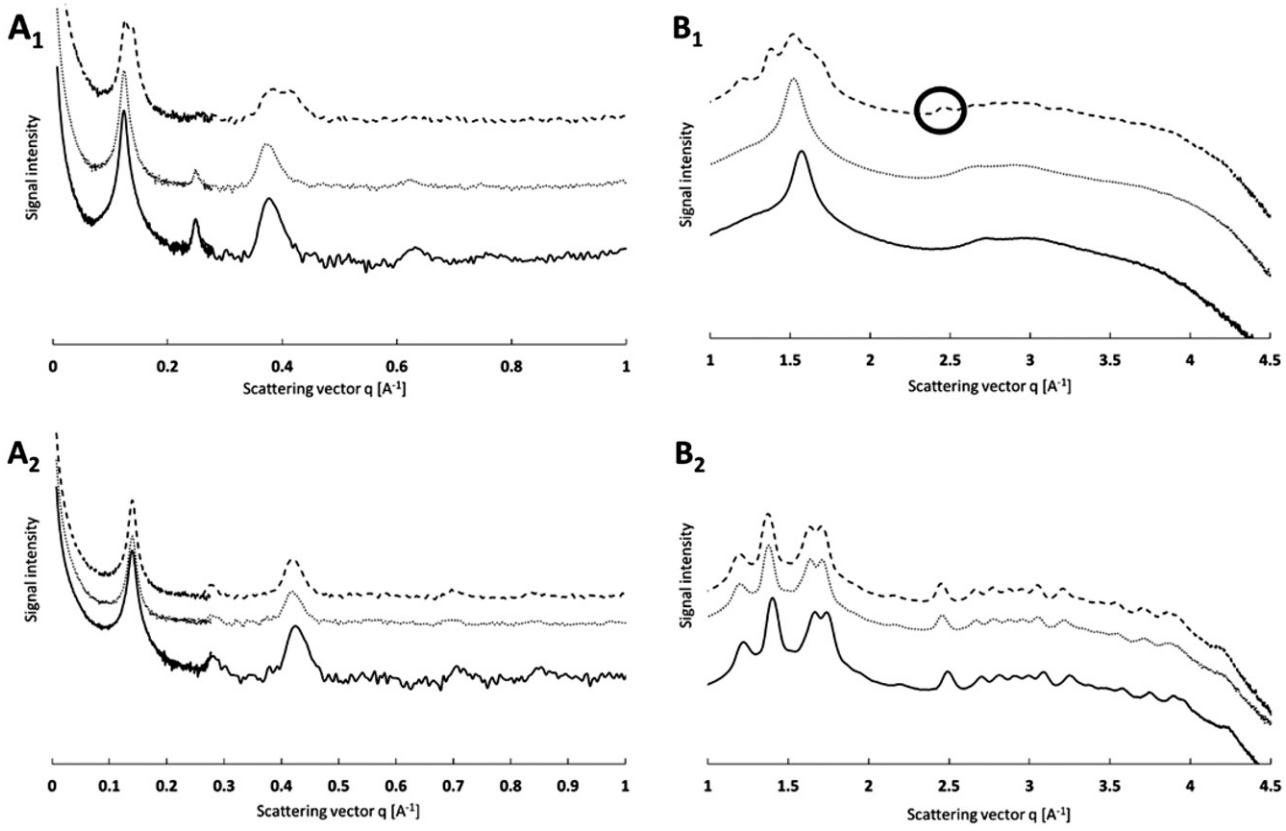

Figure 5. SAXS signal (A) and WAXS signal (B) of the microparticles without essential oil (1) and of the microparticles with 75g/kg essential oil (2) after production (—) and after 2 months storage at 25 °C (·····) or 37 °C (– –); ($n = 2$).

Table 2. Summary of the effects of essential oil concentration and storage on the physico-chemical properties of fat-based microparticles.

	No essential oil	Essential oil concentration $\leq$75 g kg^{-1}	Essential oil concentration $\geq$75 g kg^{-1}
Crystalline structure	α- or β′-form after production; Transformation to stable β-form throughout storage at 37 °C	β-form directly after production; Constant throughout storage	
Melting behaviour	Two distinct melting steps; Enthalpy shift towards higher temperature throughout storage	Constant melting profiles throughout storage	
Surface structure	Development of fat blooming throughout storage	Occurrence of fat blooming directly after production	Microparticle surfaces mostly free from fat blooming
Storage and effect on product applicability	Agglomeration when stored at 37 °C; Application as free flowing powder only after the impact of mechanical force	Agglomeration when stored at 25 or 37 °C; Application as free flowing powder only after the impact of mechanical force	Free-flowing powder throughout storage

Addition of 75–300 g/kg essential oil to microparticles made from hydrogenated vegetable oil accelerates the polymorphic transition of the fat and stabilises its crystalline state throughout storage at 25 °C and 37 °C. The appearance of fat blooming on the surface of microparticles with 75 g/kg essential oil was not a result of polymorphic transformation of the triglycerides but was probably a result of fat migration through the semi-solid matrix and its recrystallization at the surface of the microparticles. When the essential oil concentration exceeds a certain value, this effect is suppressed.

Transition to the most stable polymorphic form in the presence of essential oil occurred within the first 24 h after production of the microparticles. During subsequent storage, no changes in the melting behaviour of the microparticles have to be expected.

The main outcomes summarising all investigated physico-chemical properties over a storage time of up to 2 months are summarised in Table 2.

4. Conclusion

Microparticles without essential oil experienced obvious, storage time, and temperature-dependent changes in their physico-chemical properties. For the essential oil containing microparticles, the physico-chemical properties were constant under the applied storage conditions. When the essential oil concentration was below or equal to 75 g/kg microparticles tended to form fat blooming on their surface and transformed into robust agglomerates during storage. In case the essential oil concentration exceeded a certain level the products remained free flowing throughout 2 months. Due to their high essential oil content the flowability of these microparticles was generally worse.

Disclosure statement

No potential conflict of interest was reported by the authors.

Funding

This study was supported by the BIOMIN Holding GmbH. The authors want to thank BIOMIN for their financial and scientific support.

ORCID

Denis Poncelet http://orcid.org/0000-0003-3191-0210
Stephen Cole http://orcid.org/0000-0001-9618-4606

References

Arun, P., *et al.*, 2011. Evaluation of hot melt coating as taste masking tool. *International research journal of pharmacy*, 2, 169–172.

Bento, M.H.L., *et al.*, 2013. Essential oils and their use in animal feeds for monogastric animals-effects on feed quality, gut microbiota, growth performance and food safety: a review. *Veterinarni medicina*, 58 (No. 9), 449–458.

Blake, A., and Attwool, P., 1998. Particulate flavor compositions and process to prepare same. Canadian Patent 2177, 384C.

Bricknell, J., and Hartel, R.W., 1998. Relation of fat bloom in chocolate to polymorphic transition of cocoa butter. *Journal of the American oil chemists' society*, 75 (11), 1609–1615.

De Graef, V., *et al.*, 2005. Prediction of migration fat bloom on chocolate. *European journal of lipid science and technology*, 107 (5), 297–306.

Dewettinck, K., and Huyghebaert, A., 1999. Fluidized bed coating in food technology. *Trends in food science & technology*, 10, 163–168.

Dolçà, C., *et al.*, 2015. Microencapsulation of rosemary essential oil by co-extrusion/gelling using alginate as a wall material. *Journal of encapsulation and adsorption sciences*, 05 (03), 121–130.

El Asbahani, A., *et al.*, 2015. Essential oils: from extraction to encapsulation. *International journal of pharmaceutics*, 483 (1-2), 220–243.

Gibbs, F., *et al.*, 1999. Encapsulation in the food industry: a review. *International journal of food sciences and nutrition*, 50 (3), 213–224.

Gottschalk, P., *et al.*, 2018. Formation of essential oil containing microparticles comprising a hydrogenated vegetable oil matrix and characterisation thereof. *Journal of microencapsulation*, 1, 26.

Himawan, C., Starov, V., and Stapley, A., 2006. Thermodynamic and kinetic aspects of fat crystallization. *Advances in colloid and interface science*, 122 (1-3), 3–33.

Jozwiakowski, M.J., Jones, D.M., and Franz, R.M., 1990. Characterization of a hot-melt fluid bed coating process for fine granules. *Pharmaceutical research*, 07 (11), 1119–1126.

Jyothi, N.V.N., *et al.*, 2010. Microencapsulation techniques, factors influencing encapsulation efficiency. *Journal of microencapsulation*, 27 (3), 187–197.

Jyothi, S., *et al.*, 2012. Microencapsulation: a review. *International journal of pharmacy and biological sciences*, 3, 509–531.

Kausadikar, S., Gadhave, A.D., and Waghmare, J., 2015. Microencapsulation of lemon oil by spray drying and its application in flavour tea. *Advances in applied science research*, 6, 69–78.

Lopes, D.G., *et al.*, 2015. Role of lipid blooming and crystallite size in the performance of highly soluble drug-loaded microcapsules. *Journal of pharmaceutical sciences*, 104 (12), 4257–4265.

Lumay, G., *et al.*, 2012. Measuring the flowing properties of powders and grains. *Powder technology*, 224, 19–27.

Martins, I.M., *et al.*, 2009. Microencapsulation of thyme oil by coacervation. *Journal of microencapsulation*, 26 (8), 667–675.

Mayama, H., 2009. Blooming theory of tristearin. *Soft matter*, 5 (4), 856–859.

Miyasaki, E.K., *et al.*, 2016. Acceleration of polymorphic transition of cocoa butter and cocoa butter equivalent by addition of d-limonene. *European journal of lipid science and technology*, 118 (5), 716–723.

Murugesan, G.R., *et al.*, 2015. Phytogenic feed additives as an alternative to antibiotic growth promoters in broiler chickens. *Frontiers in veterinary science*, 2, 21.

Nassu, R.T., and Gonçalves, L.A.G., 1999. Determination of melting point of vegetable oils and fats by differential scanning calorimetry (DSC) technique. *Grasas y aceites*, 50 (1), 16–21.

Nedovic, V., *et al.*, 2011. An overview of encapsulation technologies for food applications. *Procedia food science*, 1, 1806–1815.

Okuro, P.K., de Matos Junior, F.E., and Favaro-Trindade, C.S., 2013. Technological challenges for spray chilling

encapsulation of functional food ingredients. *Food technology and biotechnology*, 51, 171–182.

Rigolle, A., *et al.*, 2016. Isothermal crystallization behavior of cocoa butter at 17 and 20°C with and without limonene. *Journal of agricultural and food chemistry*, 64 (17), 3405–3416.

Sato, K., 2001. Crystallization behaviour of fats and lipids—a review. *Chemical engineering science*, 56 (7), 2255–2265.

Schoenitz, M., *et al.*, 2014. Controlled polymorphic transformation of continuously crystallized solid lipid nanoparticles in a microstructured device: a feasibility study. *European journal of pharmaceutics and biopharmaceutics*, 86 (3), 324–331.

Suresh, G., *et al.*, 2018. Alternatives to antibiotics in poultry feed: molecular perspectives. *Critical reviews in microbiology*, 44 (3), 318–335.

Takeuchi, M., Ueno, S., and Sato, K., 2002. Crystallization kinetics of polymorphic forms of a molecular compound constructed by SOS (1, 3-distearoyl-2-oleoyl-sn-glycerol) and SSO (1, 2-distearoyl-3-oleoyl-rac-glycerol). *Food research international*, 35 (10), 919–926.

Turasan, H., Sahin, S., and Sumnu, G., 2015. Encapsulation of rosemary essential oil. *LWT-Food science and technology*, 64 (1), 112–119.

Vervaeck, A., *et al.*, 2013. Prilling of fatty acids as a continuous process for the development of controlled release multiparticulate dosage forms. *European journal of pharmaceutics and biopharmaceutics*, 85 (3), 587–596.

Yang, J., and Ciftci, O.N., 2016. Development of free-flowing peppermint essential oil-loaded hollow solid lipid micro- and nanoparticles via atomization with carbon dioxide. *Food research international*, 87, 83–91.

Zeng, Z., *et al.*, 2015. Essential oil and aromatic plants as feed additives in non-ruminant nutrition: a review. *Journal of animal science and biotechnology*, 6 (1), 7.

Ziegleder, G., and Schwingshandl, I., 1998. Kinetics of fat migration within chocolate products. Part III: Fat bloom. *Lipid – Fett*, 100 (9), 411–415.